



# Mechanical properties of Japanese black pine (*Pinus thunbergii* Parl.) planted on coastal sand dunes: resistance to uprooting and stem breakage by tsunamis

Kazuki Nanko<sup>1</sup> · Satoru Suzuki<sup>1</sup> · Hironori Noguchi<sup>2</sup> · Yoji Ishida<sup>3</sup> · Delphis F. Levia<sup>4,5</sup> · Akira Ogura<sup>6</sup> · Hiroaki Hagino<sup>2</sup> · Hiroshi Matsumoto<sup>3</sup> · Hiromi Takimoto<sup>7</sup> · Tomoki Sakamoto<sup>1</sup>

Received: 26 October 2016 / Published online: 15 February 2019  
© Springer-Verlag GmbH Germany, part of Springer Nature 2019

## Abstract

Given that Japanese black pine trees (*Pinus thunbergii* Parl.) are predominant in the coastal forests of Japan and are part of the defence structure against tsunamis, the quantification of their resistance to tree damage is necessary. The resistance of Japanese black pine to uprooting and stem breakage and its bending properties were estimated by a tree-pulling test and bending test of green logs in conjunction with the published literature. A general equation to estimate the critical turning moment for uprooting was developed using diameter at breast height and tree height as predictor variables. For moduli of elasticity and rupture of stems (MOE and MOR), medians [5th and 95th percentile values] were 5.41 [3.78, 6.82] GPa and 35.0 [28.7, 41.8] MPa, respectively. With the obtained critical turning moment and MOR, the critical tsunami water depth was estimated by numerical simulations using modelled trees. The numerical simulations revealed that Japanese black pine trees on coastal sand dunes tended to be more vulnerable to uprooting than stem breakage, with taller and more slender trees showing less resistance to stem breakage. The results on the mechanical properties of Japanese black pine are of use to those in the wood science community as well as coastal managers who need to know the mechanical strength of Japanese black pine to help evaluate their resistance against tsunamis.

## Introduction

Study on the response of trees to stress has taken many different vantage points. Some studies have examined the effects of insect stressors (e.g. Kimmins 1972; Hollinger 1986; Konta 2001), drought (e.g. Williams et al. 2013) or forest management (Pretzsch and Rais 2016) on trees and forests. Other studies have focused

---

✉ Kazuki Nanko  
knanko@ffpri.affrc.go.jp

Extended author information available on the last page of the article

on the mechanical strength of wood and examined the effects of air temperature (Schmidt and Pomeroy 1990; Silins et al. 2000), ice storms (Lemon 1961; Seischab et al. 1993; Nock et al. 2016), snow capping (Cannell and Morgan 1989; Kinar and Pomeroy 2015) and wind (e.g. Merrill 1948; Bascañán et al. 2006; Auty and Achim 2008) on tree trunk and/or branch bending or breakage. The structural analysis of tree trunks and branches has also been utilized to better understand the effects of complex loading on deflection (Morgan and Cannell 1987). A thorough and comprehensive understanding of the physical breakage of tree branches and stems is important from many perspectives, ranging from the development or validation of theories on the mechanical properties of wood to the management of forest buffer zones.

Coastal forests play a vitally important role in mitigating the deleterious effects of strong wind, blown sand, airborne salt and tsunamis (Murai et al. 1992; Suzuki et al. 2016). The protective role of coastal forests against tsunamis has attracted concerted attention since the 1998 Papua New Guinea tsunami (Dengler and Preuss 2003), the 2004 Indian Ocean tsunami (Danielsen et al. 2005; Forbes and Broadhead 2007; Rossetto et al. 2007), and the tsunami caused by the Great East Japan Earthquake in 2011 (Tanaka et al. 2013; FFPRI 2015). On the other hand, coastal forests are sometimes destroyed by tsunamis. To evaluate the effect of coastal forests as a part of multi-defence structure against tsunamis, the quantification of their resistance to tree damage is necessary. In Japan, Japanese black pine (*Pinus thunbergii* Parl.) is the most popular species for planting in these shelterbelt coastal forests because of its ability to grow in the most severe coastal environments and persist, despite sand saltation and salt exposure (Oda 2003; Nakashima and Okada 2011; Suzuki et al. 2016). Few studies, however, have been conducted on estimating the resistance of Japanese black pine to tree damage.

There are two main types of tree damage by a tsunami: uprooting and stem breakage (Tanaka et al. 2013). The resistance to uprooting is determined from root-soil plate anchorage, which in turn depends on the root-soil plate weight, depth and diameter of the root-soil plate, as well as the soil properties (Coutts 1986; Peltola et al. 1999). The root anchorage is influenced by soil and rooting conditions (Nicoll et al. 2006), but no direct evidence for a reduction in the resistance due to soil saturation can be detected because the additional weight of the water in the soil compensates for any loss of soil strength (Gardiner et al. 2016). Since it is difficult to estimate the weight and the size of a root-soil plate non-destructively, the root anchorage is estimated by aboveground tree size, such as stem diameter at breast height ( $D_{BH}$ ), tree height ( $H_{tr}$ ) and stem mass, with the results from tree-pulling tests (Peltola et al. 2000; Nicoll et al. 2006; Kamimura et al. 2012). From the tree-pulling tests, the critical turning moment at the stem breakage point is obtained. When the tree is uprooted, the stem breakage point is assumed at the tree base. In general, larger trees have larger root anchorage due to larger root-soil plates. Previous studies have estimated the critical turning moment by power regression with  $D_{BH}$  (e.g. Fukami et al. 2011), linear regression with  $H_{tr} \times D_{BH}^2$  (e.g. Cucchi et al. 2004; Peltola et al. 2000; Todo et al. 2015) or linear regression with stem mass (e.g. Achim et al. 2005; Gardiner et al. 2000). The stem mass is mechanistically the best-fit variable to estimate the critical turning moment (Peterson and Claassen 2013); however, it is a difficult quantity to

obtain non-destructively. Therefore,  $D_{BH}$  and  $H_{tr}$  are the most accessible predictors to estimate a tree's resistance to uprooting.

Despite the dominance of Japanese black pine trees in these coastal forests, rather few studies have estimated their resistance to uprooting. The existing studies on the resistance of Japanese black pine to uprooting (Imai and Suzuki 2005; Kondo et al. 2006; Ono and Ishikawa 2012; Imai et al. 2013; Miyata et al. 2013; Noguchi et al. 2014) had small sample sizes based on smaller trees and fewer trees  $> 0.2$  m in  $D_{BH}$ . Therefore, the present comprehensive estimation of the critical turning moment for Japanese black pine is based on an integration of all of the previous data from past studies plus new data from larger trees with a  $D_{BH} > 0.2$  m.

The resistance to stem breakage is determined by the bending strength of the stem. The modulus of rupture (MOR) of tree stems has been measured by bending tests as the bending strength, simultaneously obtaining the modulus of elasticity (MOE) (Koizumi 1987; Tanaka et al. 1994; Ruel et al. 2010; Ido et al. 2013). MOE and MOR vary among and within tree species, and are influenced by wood properties. For example, larger annual ring width causes lower MOE and MOR because the relative percentage of earlywood is higher (Koizumi 1987; Kato and Nakatani 2000). Cambial age is one of the variables that were found to influence the MOE because juvenile wood was more elastic than mature wood. The MOE increased with age and gradually reached a maximum (Koizumi 1987; Leban and Haines 1999; Bascuñán et al. 2006; Auty and Achim 2008; Sattler et al. 2014). In addition, MOR decreased with the number of branch knots and presence of rot (Ruel et al. 2016; Gardiner et al. 2016).

Whereas there are a litany of studies examining the bending strength and elasticity of timbers in wood science, for example, as the database summarized in Forest Products Laboratory (1999), there is a dearth of information on stem breakage from living Japanese black pine trees or green logs. Therefore, the actual measurement of MOE and MOR for green logs is necessary for estimating the resistance of Japanese black pine to stem breakage. MOR of fresh stems was measured by Imai et al. (2013) and estimated by Noguchi et al. (2014) to quantify the critical bending stress to trigger stem breakage, but the sample sizes were small with three and one trees, respectively.

There are many forces acting on structures in tsunamis (Federal Emergency Management Agency 2012), including direct hydrostatic and hydrodynamic forces from water inundation, impact forces from water-borne debris, and scour and slope/foundation failures (Tanaka et al. 2013). Numerical simulations are useful to evaluate the resistance of Japanese black pine trees against tsunamis. For example, Noguchi et al. (2012) evaluated the partial damage and the mitigation effect of the inundation flow by coastal forests composed of Japanese black pine. Tanaka et al. (2013) confirmed the efficacy of the coastal forest to trap debris (including large trees and car debris) in tsunamis by calculating critical  $D_{BH}$  of Japanese black pine trees. The influence of tree size on tree damage rate and type was verified from calculations of critical tsunami flow velocity (Torita et al. 2014). These studies confirmed the effectiveness of the numerical simulations by comparison with field surveys of damaged trees by the tsunami of the Great East Japan Earthquake in 2011. Applications of numerical

simulations better clarify the resistance of Japanese black pine trees in coastal forest to damage by tsunamis and their ability to mitigate damage.

With specific regard to Japanese black pine trees growing on coastal sand dunes, the objectives of this study were to: (1) quantify the resistance to uprooting in relation to tree size; (2) quantify the resistance to stem breakage in relation to wood properties; and (3) estimate resistance to tree damage by tsunamis through numerical simulations. By examining live trees in the field, this study will augment the database on the mechanical properties of tree strength for Japanese black pine and supply coastal managers with relevant data on the ability of Japanese black pine to survive from interactions with tsunamis.

## Materials and methods

### Tree-pulling test and estimation of the resistance to uprooting

A tree-pulling test was conducted on six Japanese black pine trees on the coastal sand dunes of Kaga National Forest (Ishikawa, Japan (36°18'N, 136°16'E)) in September 2014 to measure their resistance to uprooting. The six trees were between 89 and 98 years old, with  $D_{BH}$  ranging from 0.2 to 0.3 m and  $H_{tr}$  ranging from 10.5 to 15.3 m (Table 1). The maximum root clump depth ranged from 1.9 to 3.2 m, with a mean root clump mass of 268.1 kg (Table 1).

A soft polyester yarn sling was positioned on the tree stem between 2 and 4 m above ground and connected to a steel wire which was pulled by a backhoe until peak tensile load was confirmed (Fig. 1). Tensile load was measured by a 100-kN capacity load cell (TR2110H, Minebea, Nagano, Japan) or 20-kN capacity load cell (LUX-B-20KN-I, Kyowa Electronic Instruments, Tokyo, Japan) connected between the polyester sling and steel wire and recorded by a 100 Hz datalogger (EDS-400A, Kyowa Electronic Instruments, Tokyo, Japan) and a laptop computer. The angle between the pulled stem and vertical direction ( $\alpha$ , rad) and the angle between the tensile direction and horizontal direction ( $\beta$ , rad) were acquired from video feed positioned at a right angle to the tensile direction. After the tree-pulling tests, each stem was segmented into logs, and both the logs and foliage were subsequently weighed. In addition, the root clumps of each tree were excavated, and root mass, maximum rooting depth and length of eight root radii (every 45°) were measured.

According to Nicoll et al. (2005), the turning moment at the stem breakage point ( $M_{total}$ , N m, Eq. 1) is calculated as the sum of the turning moment by tree pulling ( $M_{pull}$ , N m, Eq. 2) and the turning moment by tree weight ( $M_{gravity}$ , N m, Eq. 3) as per the below equations:

$$M_{total} = M_{pull} + M_{gravity} \quad (1)$$

$$M_{pull} = P_T (h_p - h_b) \cos(\alpha - \beta) \quad (2)$$

$$M_{gravity} = g (h_g - h_b) \sin \alpha \int_{h_b}^h w(z) dz \quad (3)$$

**Table 1** Descriptive statistics and pulling test data for Japanese black pine trees in this study

#	Aboveground					Root clump				Pulling test					
	Age (year)	$D_{BH}$ (cm)	$D_0$ (cm)	$H_r$ (m)	$H_{cb}$ (m)	Stem volume ( $m^3$ )	Total mass (kg)	Maximum depth (m)	Mean radius (m)	Mass (kg)	Breakage type <sup>a</sup>	$h_p$ (m)	$h_g$ (m)	$h_b$ (m)	$M_{max}$ ( $10^3$ N m)
1	97	24.5	30.7	14.4	5.5	0.398	345.0	3.2	2.2	190.6	SB	3.0	5.1	0.5	55.9
2	93	20.1	25.5	10.5	2.2	0.163	249.0	1.9	3.0	202.8	U	2.0	4.1	0	38.9
3	89	28.5	29.5	11.1	3.1	0.328	576.9	2.0	2.3	319.3	U	3.1	4.1	0	79.7
4	92	30.1	36.2	15.3	4.4	0.485	728.7	2.0	3.1	384.9	U	4.0	6.0	0	102.6
5	98	23.8	29.5	11.7	4.1	0.306	397.7	2.4	3.6	267.9	U	2.2	4.6	0	69.5
6	98	28.4	31.3	14.5	3.5	0.404	527.9	2.5	2.7	243.2	U	3.0	5.3	0	85.7

$D_{BH}$  stem diameter at breast height (1.3 m),  $D_0$  stem diameter at the tree base,  $H_r$  tree height,  $H_{cb}$  the height of crown bottom,  $h_p$  height at pulling point,  $h_g$  height at centre of gravity,  $h_b$  height at broken point,  $M_{max}$  critical turning moment for tree breakage

<sup>a</sup>SB stem breakage, U uprooted

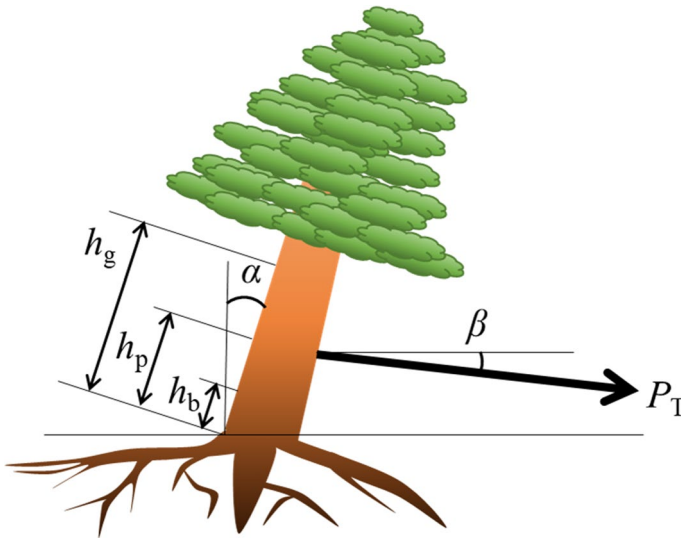


**Fig. 1** Schematic diagram of the tree-pulling test, where  $P_T$  denotes tensile load,  $\alpha$  and  $\beta$  denote the angles between the pulled stem and vertical direction and between the tensile direction and horizontal direction, respectively, and  $h_g$ ,  $h_p$ , and  $h_b$  denote the heights of centre of gravity, pulling point and stem breakage point, respectively

where  $P_T$  is tensile load (N),  $h_p$ ,  $h_b$  and  $h_g$  are the heights of pulling point (m), stem breakage point (m) and centre of gravity (m), respectively,  $g$  is the acceleration of gravity ( $\text{m s}^{-2}$ ), and  $w(z)$  is the mass of the tree at height  $z$  (m). The maximum  $M_{\text{total}}$  was considered as the critical turning moment for tree breakage ( $M_{\text{max}}$ , N m). When the tree was uprooted,  $h_b$  was zero and  $M_{\text{max}}$  was considered the critical turning moment for uprooting ( $M_{C_{\text{uproot}}}$ , N m).

The resistance of Japanese black pine trees to uprooting was estimated by  $M_{C_{\text{uproot}}}$  based on a combination of current experimental results and the past literature with similar pulling tests on Japanese black pine trees inhabiting coastal dunes (Table 2; Imai and Suzuki 2005; Kondo et al. 2006; Ono and Ishikawa 2012; Imai et al. 2013; Miyata et al. 2013; Noguchi et al. 2014). The resistance to uprooting is normally predicted from the estimate of the root-soil plate weight (Peltola et al. 1999) or stem weight (Gardiner et al. 2000); however, these data were insufficient from the data set.  $M_{C_{\text{uproot}}}$  was estimated by a power regression with  $D_{\text{BH}}$  using 71 samples and a linear regression with  $H_{\text{tr}} \times D_{\text{BH}}^2$  using 46 samples.

### Bending test and the resistance to stem breakage

Fifteen straight stem logs from differing heights and eight straight coarse root sections were sampled from the pulled trees to measure both the MOE and MOR within 7 days of the pulling test. The pulled trees were covered with plastic sheets to minimize desiccation. Straight coarse root sections were preferentially selected

**Table 2** Tree size and critical turning moment of Japanese black pine trees on coastal sand dunes gained by tree-pulling tests in this study and the past literature

	Number of trees	$D_{BH}$ (cm)	$H_{tr}$ (m)	$M_{C_{uproot}}$ ( $10^3$ N m)
This study	5	20.1–30.1	10.5–15.3	38.9–102.6
Imai and Suzuki 2005	18	6.5–13.2	5.5–11.5	1.5–10.6
Kondo et al. 2006	5	10.7–22.9	9.1–13.9	6.8–65.1
Ono and Ishikawa 2012	12	14.0–40.3	NA	7.6–198.7
Imai et al. 2013	15	8.1–22.0	6.0–13.3	1.7–49.2
Miyata et al. 2013	13	15.7–29.2	NA	23.7–98.0
Noguchi et al. 2014	3	9.0–13.7	4.8–6.9	2.7–12.6
Total or range	71	6.5–40.3	4.8–15.3	1.5–198.7

$D_{BH}$  stem diameter at breast height (1.3 m),  $H_{tr}$  tree height,  $M_{C_{uproot}}$  critical turning moment for uprooting

because the straight samples were desirable for the bending test. Sample properties are summarized in Table 3. Bending properties were measured using a universal testing machine of 1000-kN capacity (UH-1000kNXR, SHIMADZU, Kyoto, Japan). For purposes of computation, all of the logs were considered to represent tapered cylinders to calculate volume and wood density. Three-point bending tests (Fig. 2) were conducted on the selected logs. Since no standard exists for such tests, the bending tests for round timber described in Ido et al. (2013) were followed. The MOE was calculated by Eq. 4 considering the effect of taper, according to Sawada (1983):

$$MOE = \frac{Pl^3}{48I_m \delta_m} \frac{(1+\tau)^2}{4\tau} = \frac{Pl^3}{3\pi D_m^4 \delta_m} \frac{(1+\tau)^2}{4\tau} \quad (4)$$

$$\tau = \frac{D_1}{D_2} \quad (5)$$

where  $P$  is load (N),  $l$  is the length between two supporting points (m),  $I_m$  is the second moment of area at the mid-span ( $m^4$ ),  $\delta_m$  is the deflection of the mid-span (m),  $D_m$  is the mean diameter at the mid-span,  $\tau$  is taper, and  $D_1$  and  $D_2$  are the mean diameters at thicker and thinner supporting points, respectively. Six displacement gauges (SDP-200D and CDP-100, Tokyo Sokki Kenkyujo Co., Ltd., Tokyo, Japan) were used to measure  $\delta_m$ . The displacement of both sides of a log at two supporting points and a compression point were measured. The MOR was calculated by Eq. 6 considering the effect of taper:

$$MOR = \frac{Pl}{4Z_m} \frac{(1+\tau)^2}{4\tau} = \frac{2Pl}{D_m} \frac{(1+\tau)^2}{\tau} \quad (6)$$

where  $Z_m$  is the section modulus at the mid-span ( $m^3$ ). After the bending test, a disc (~3 cm thick) was extracted at 20 cm from the bending point in the thinner direction

**Table 3** Modulus of elasticity (MOE) and modulus of rupture (MOR) of stem logs and coarse root sections for Japanese black pine from the bending test

Tree #	Log			Disc <sup>a</sup>				Mechanical property				
	$D_m$ (cm)	$\tau$	$L$ (m)	$I$ (m)	$H_C$	$\rho_{w\_fresh}$ ( $kg\ m^{-3}$ )	$\rho_{w\_dry}$ ( $kg\ m^{-3}$ )	Cambial age (year)	ARW (mm)	MC (%)	MOE (GPa)	MOR (MPa)
<i>Stem</i>												
1	16.2	0.645	4.02	3.6	0.493	979.7	377.9	30	2.40	159.3	4.76	28.3
1	8.9	0.454	2.64	1.8	0.264	908.5	399.6	17	2.53	127.4	5.43	33.1
1	5.0	0.667	1.27	0.9	0.132	1069.8	475.3	8	2.69	125.1	5.41	42.2
2	13.9	0.640	3.65	2.7	0.586	1064.9	466.1	23	2.81	128.5	6.44	39.7
2	9.2	0.575	2.21	1.8	0.314	1124.6	476.1	12	3.30	136.2	4.04	30.0
2	4.6	0.613	1.23	0.9	0.105	992.6	384.7	6	3.24	158.0	3.16	41.6
3	9.6	0.278	3.04	1.8	0.279	1160.1	461.0	12	3.21	151.6	4.17	30.8
4	25.2	0.636	6.07	5.4	0.719	1020.1	451.4	62	1.94	126.0	6.42	35.0
4	14.8	0.492	4.06	2.7	0.392	1108.0	470.9	17	4.05	135.3	6.24	39.2
4	6.6	0.394	2.06	1.8	0.196	831.0	328.5	7	4.82	152.9	4.76	34.4
5	15.1	0.511	4.00	3.6	0.462	876.4	383.9	21	3.33	128.3	7.15	40.2
5	22.2	0.724	4.31	4.0	0.816	797.0	337.9	63	1.58	135.8	6.42	35.5
6	18.6	0.778	4.23	3.6	0.566	976.3	401.0	24	3.69	143.5	6.68	36.6
6	13.8	0.594	3.22	2.7	0.310	1100.7	418.7	15	4.33	162.9	4.99	30.4
6	6.5	0.334	2.01	1.8	0.131	1002.6	388.2	8	3.24	158.3	4.08	28.9
Median	13.8	0.594				1002.6	401.0	17.0	3.24	136.2	5.41	35.0
5th percentile	4.9	0.317				820.8	335.1	6.7	1.83	125.7	3.78	28.7
95th percentile	4.9	0.740				1135.3	475.5	62.3	4.48	160.4	6.82	41.8
<i>Root</i>												
1	8.8	0.782	1.69	0.9		870.2	499.7	26	1.51	74.1	7.94	49.9
2	12.5	0.749	1.56	0.9		967.8	528.3	27	2.20	83.2	5.93	49.7



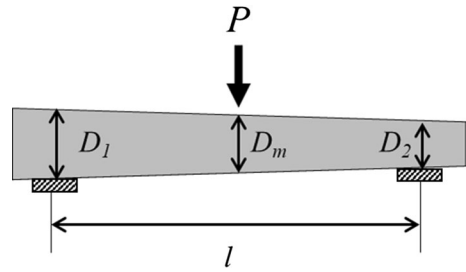
Table 3 (continued)

Tree #	Log				Disc <sup>a</sup>			Mechanical property			
	$D_m$ (cm)	$\tau$	$L$ (m)	$l$ (m)	$H_C$	$\rho_{W\_fresh}$ ( $kg\ m^{-3}$ )	$\rho_{W\_dry}$ ( $kg\ m^{-3}$ )	ARW (mm)	MC (%)	MOE (GPa)	MOR (MPa)
2	11.1	0.650	1.02	0.9		881.4	500.3	1.81	76.2	3.83	32.3
3	5.1	0.622	1.61	0.9		923.3	515.2	1.08	79.2	2.02	36.1
4	7.1	0.653	1.52	0.9		909.5	474.3	1.53	91.7	12.66	48.7
5	6.0	0.924	1.86	1.8		1036.6	571.6	2.32	81.4	5.45	44.2
6	12.0	0.463	2.22	1.8		1068.5	532.0	1.84	100.8	6.94	46.0
6	3.9	0.664	0.96	0.9		908.7	535.1	1.55	69.8	9.29	64.4
Median	8.0	0.659				916.4	521.8	1.68	80.3	6.44	47.4
5th percentile	4.3	0.519				874.1	483.2	1.23	71.3	2.65	33.6
95th percentile	12.3	0.874				1057.3	558.8	2.28	97.6	11.48	59.3

$D_m$  mean diameter at the mid-span,  $\tau$ -taper,  $L$  length of the stem log or coarse root section,  $l$  length between supporting points,  $H_C$  relative height from tree top to the mid-span,  $\rho_{W\_fresh}$  fresh wood density,  $\rho_{W\_dry}$  dry wood density, ARW average annual ring width, MC moisture content, MOE modulus of elasticity, MOR modulus of rupture

<sup>a</sup>Disc was sampled at 20 cm from the bending point of the log in the direction of log taper

**Fig. 2** Schematic diagram of the bending test, where  $P$  denotes load,  $l$  denotes the length between two supporting points, and  $D_m$ ,  $D_1$ , and  $D_2$  denote the mean diameters of the span centre, at the thicker supporting point and at the thinner supporting point, respectively



of the log. From the disc, cambial age, average annual ring width and moisture content (by the oven-dry method) were determined.

### Estimation of the resistance to tree damage against tsunamis

To estimate the resistance to tree damage against tsunamis, a numerical simulation for modelled trees was conducted. Two different tree shapes were created with  $H_{tr}/D_{BH}$  values of 50 and 70, respectively, with  $H_{tr}$  ranging from 2 to 16 m. Stem profiles of the modelled trees were determined by the Behre hyperbola (Bruce 1972) in Eq. 7 as:

$$D' = \frac{L'}{a+bL'} \quad (7)$$

where  $D'$  is relative stem diameter standardized by diameter at  $L'=0.9$ ,  $L'$  is relative tree length from the tree top standardized by  $H_{tr}$ , and  $a$  and  $b$  are constants chosen to match a tree's general profile. Thus, stem diameter at height  $z$  ( $D(z)$ , m) was calculated in Eq. 8 as:

$$D(z) = D(0.1H_{tr}) \frac{H_{tr}^{-z}}{a+b \frac{H_{tr}^{-z}}{H_{tr}}} \quad (8)$$

where  $D(0.1H_{tr})$  was calculated in Eq. 9 with  $D_{BH}$  and  $H_{tr}$  as:

$$D(0.1H_{tr}) = D_{BH} \frac{a+b \frac{H_{tr}^{-1.3}}{H_{tr}}}{\frac{H_{tr}^{-1.3}}{H_{tr}}} \quad (9)$$

Based on data from the five pulled trees (Table 1),  $a=0.590$  and  $b=0.344$  were applied, respectively, by the least-squares method (Fig. 3). Tree #3 was not used, because the tree was forked at 3.6 m. The horizontal projected area of the stem less than height  $z$  [ $0 \leq z \leq H_{tr}$ ] ( $S_{st}(z)$ , m<sup>2</sup>) was calculated as:

$$S_{st}(z) = \int_0^z D(z) dz \quad (10)$$

The crown profile of the trees was assumed to be of circular cone shape. Thus, the horizontal projection areas of the trees were triangular. A crown length of  $0.7H_{tr}$

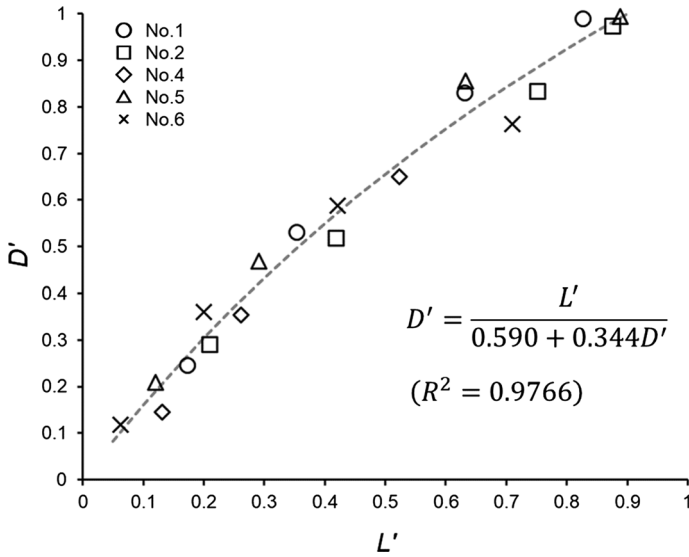


**Fig. 3** Relationship between relative stem diameter ( $D'$ ) and relative tree length from the tree top ( $L'$ ) of five Japanese black pine trees in this study. Dashed line indicates regression curve shown in Eq. 7

was applied as determined from the six pulled trees (Table 1), and thus the height of crown bottom ( $H_{cb}$ , m) was  $0.3H_{tr}$ . Total projected branch areas ( $A_{br}$ ,  $m^2$ ) or needle areas ( $A_{nd}$ ,  $m^2$ ) of a tree were estimated  $D(H_{cb})$  using the following equations for Japanese black pine derived from Noguchi et al. (2012):

$$A_{br} = 32D(H_{cb})^{1.7} \tag{11}$$

$$A_{nd} = 813D(H_{cb})^{2.4} \tag{12}$$

where  $D(H_{cb})$  was calculated from Eq. 8. The branch and needles were uniformly distributed within the canopy crown area. The horizontal projected branch and needle areas lower than height  $z$ , i.e. submerged by a tsunami (Fig. 4:  $S_{br}$  and  $S_{nd}$ , respectively,  $m^2$ ), were calculated as:

$$S_{br}(z) = \begin{cases} 0 & [z \leq H_{cb}] \\ A_{br} \left( 1 - \frac{(H_{tr}-z)^2}{(H_{tr}-H_{cb})^2} \right) & [H_{cb} < z \leq H_{tr}] \\ A_{br} & [z > H_{tr}] \end{cases} \tag{13}$$

$$S_{nd}(z) = \begin{cases} 0 & [z \leq H_{cb}] \\ A_{nd} \left( 1 - \frac{(H_{tr}-z)^2}{(H_{tr}-H_{cb})^2} \right) & [H_{cb} < z \leq H_{tr}] \\ A_{nd} & [z > H_{tr}] \end{cases} \tag{14}$$

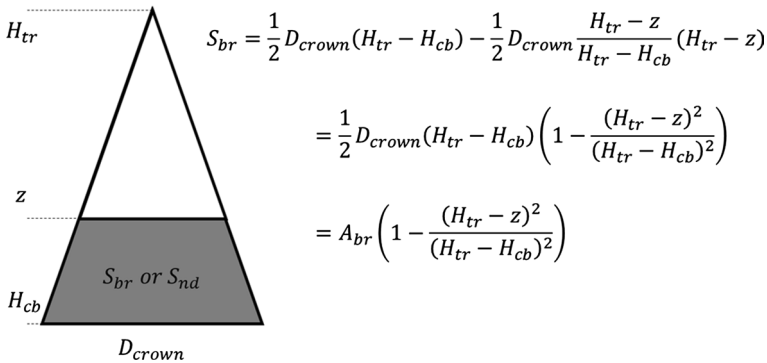


**Fig. 4** Horizontal projected areas of submerged branches and needles ( $S_{br}$  and  $S_{nd}$ , respectively) by tsunami of height  $z$  calculated by crown diameter ( $D_{crown}$ ), tree height ( $H_{tr}$ ), height of crown bottom ( $H_{cb}$ ). Total projected branch area is  $A_{br}$

For the hydrodynamic forces due to water inundation by tsunamis ( $F$ ), the resultant force acting on a tree is (Tanaka et al. 2013):

$$F = F_{drag} + F_{impulse} = (1 + k_{di})F_{drag} \tag{15}$$

where  $F_{drag}$  is drag force,  $F_{impulsive}$  is impulsive force caused by the leading edge of a surge of water impacting a tree, and  $k_{di}$  is the ratio of impulsive force to drag force. For  $k_{di}$ , a value of 1.5 was assigned in accordance with Federal Emergency Management Agency (2012) and Tanaka et al. (2013). Further, uniform water flow was applied with no vertical velocity gradient for a tsunami in accordance with Torita et al. (2014). The drag force by tsunami with a certain water height ( $H_w$ , m) to a tree was separately calculated with tsunami loads to stem ( $F_{st}$ ), branches ( $F_{br}$ ) and needles ( $F_{nd}$ ) by Eqs. 16–18 according to Tanaka et al. (2013) and Torita et al. (2014):

$$F_{st}(z) = \frac{1}{2}(1 + k_{di})\rho u^2 S_{st}(z)C_{D_{st}} = \frac{1}{2}(1 + k_{di})(Fr)^2 \rho g H_{ts} S_{st}(z)C_{D_{st}} \tag{16}$$

$$F_{br}(z) = \frac{1}{2}(1 + k_{di})\rho u^2 S_{br}(z)C_{D_{br}} = \frac{1}{2}(1 + k_{di})(Fr)^2 \rho g H_{ts} S_{br}(z)C_{D_{br}} \tag{17}$$

$$F_{nd}(z) = \frac{1}{2}(1 + k_{di})\rho u^2 S_{nd}(z)C_{D_{nd}} = \frac{1}{2}(1 + k_{di})(Fr)^2 \rho g H_{ts} S_{nd}(z)C_{D_{nd}} \tag{18}$$

where  $\rho$  is water density ( $= 999.97 \text{ kg m}^{-3}$ ),  $u$  is flow velocity ( $\text{m s}^{-1}$ ) and  $Fr$  is the Froude number ( $= u / \sqrt{gH_{ts}}$ ).  $Fr$  determines the relationship between flow water depth and flow velocity. 0.7 and 1.0 were applied for  $Fr$  because Tanaka et al. (2013) reported (from the previous literature) that  $Fr$  of most of the tsunami flow to be between 0.7 and 1.0. 0.85, 0.81 and 0.056 were applied for the drag coefficients of stem ( $C_{D_{st}}$ ), branch ( $C_{D_{br}}$ ) and needle ( $C_{D_{nd}}$ ) of Japanese black pine, respectively, as derived from Noguchi et al. (2012).

The turning moment of the stem at height  $z$  in water flow,  $M(z)$ , was calculated by the below equations as:

$$M(z) = M_{st}(z) + M_{br}(z) + M_{nd}(z) \quad (19)$$

$$M_{st}(z) = (F_{st}(H_W) - F_{st}(z))H_{gst}(H_W, z) \quad (20)$$

$$M_{br}(z) = (F_{br}(H_W) - F_{br}(z))H_{gbr}(H_W, z) \quad (21)$$

$$M_{nd}(z) = (F_{nd}(H_W) - F_{nd}(z))H_{gnd}(H_W, z) \quad (22)$$

where  $H_{gst}(H_W, z)$ ,  $H_{gbr}(H_W, z)$ , and  $H_{gnd}(H_W, z)$  is height of the centre of gravity of stem, branches and needles in water flow between  $z$  and  $H_W$ , respectively. The turning moment at the tree base was  $M(0)$ . Bending stress of the stem at height  $z$  in water flow,  $\sigma(z)$ , was calculated by Eq. 23, following Noguchi et al. (2012), as:

$$\sigma(z) = \frac{|M(z)|}{Z(z)} = \frac{32|M(z)|}{\pi D(z)^3} \quad (23)$$

where  $Z_z$  is the section modulus of stem at height  $z$ .

Critical tsunami water depth for tree damage was calculated by the balance between the tsunami load and the resistance of trees. The balance between  $M(0)$  and  $M_{C_{uproot}}$  was used for uprooting and that between  $\sigma(z)$  and MOR was used for tree breakage. In the calculations, variations for both  $M_{C_{uproot}}$  and MOR were applied. A range of  $\pm 30\%$  of  $M_{C_{uproot}}$  was used to account for the variation of root-soil anchorage related to soil conditions. 5th and 95th percentile values of MOR values from the bending tests were applied for stem bending strength to consider the variation of wood properties.

## Statistical analysis

All statistical analyses were calculated using the R software package, version 3.3.1 (R Core Team 2016). A one-way analysis of variance (ANOVA) was used to test the differences between two groups. The significance of correlations among variables was examined by the Spearman rank method. The performance of regression models was evaluated by  $R^2$  calculated as follows:

$$R^2 = \frac{[\text{cov}(\hat{y}_i, y_i)]^2}{\text{var}(\hat{y}_i)\text{var}(y_i)} \quad (24)$$

where  $\hat{y}_i$  and  $y_i$  are the predicted and observed values, respectively.

## Results and discussion

### Resistance to uprooting

In the tree-pulling test, one tree (tree #1) experienced stem breakage at a height of 0.5 m, while the other five trees were uprooted (Table 1). Thus, tree #1 was

eliminated from the analysis on uprooting resistance. A combination of the present experimental results and those of previous studies (Table 2) shows that  $M_{C_{uproot}}$  increases with  $D_{BH}$  and  $H_{tr} \times D_{BH}^2$  (Fig. 5). The following relationships were found between  $M_{C_{uproot}}$  and  $D_{BH}$  and  $H_{tr}$ :

$$M_{C_{uproot}} = 2.22 \times 10^6 D_{BH}^{2.63} \quad (R^2 = 0.949) \tag{25}$$

$$M_{C_{uproot}} = 8.09 \times 10^4 H_{tr} D_{BH}^2 \quad (R^2 = 0.964) \tag{26}$$

The 95% prediction interval of  $M_{C_{uproot}}$  had a range of  $\pm 11\,242$  N m as calculated from Eq. 26 (Fig. 5b).

### Wood properties and resistance to stem breakage

Table 3 summarizes the bending properties of the stem logs and coarse root sections. The coarse root sections were relatively more rigid than the stem logs. The stem logs had significantly lower dry wood density ( $p < 0.001$ ), larger average annual ring widths ( $p < 0.001$ ), higher moisture content ( $p < 0.001$ ) and lower MOR values ( $p = 0.001$ ) than the coarse root sections, whereas no significant differences were found for  $D_m$ , taper, cambial age, fresh wood density and the MOE between the stem logs and coarse root sections.

For stem logs, medians [5th and 95th percentile values] of MOE and MOR were 5.41 [3.78, 6.82] GPa and 35.0 [28.7, 41.8] MPa, respectively. The MOR in the study was similar to previous studies (Imai et al. 2013; Noguchi et al. 2014).

Table 4 summarizes the correlation coefficients among wood properties. Both stem logs and coarse root sections had significant positive correlations between cambial age and  $D_m$  ( $p < 0.001$ ). Older stem logs and coarse root sections were thicker objects. MOE and MOR were significantly positively correlated for the coarse root sections ( $p = 0.028$ ) but not for the stem logs. With regard to the stem logs, MOE

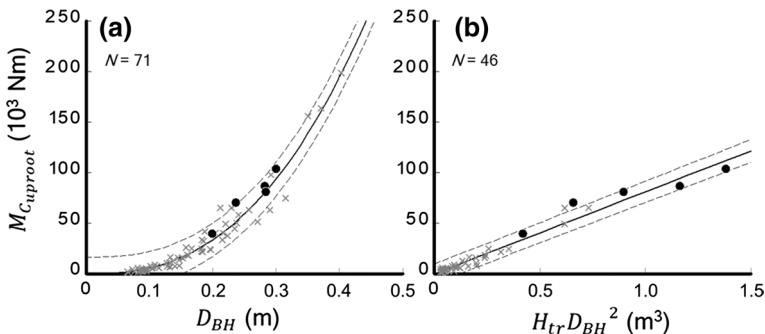


**Fig. 5** Critical turning moment for uprooting ( $M_{C_{uproot}}$ ) of Japanese black pine on coastal sand dunes related to diameter at breast height ( $D_{BH}$ ) and tree height ( $H_{tr}$ ) in this study (circle) and previous studies (cross). Solid line indicates regression expression in Eqs. 25 and 26, and dashed line indicates 95% prediction interval generated by a combination of this study and previous studies

was significantly correlated with cambial age ( $p=0.028$ ),  $D_m$  ( $p=0.0049$ ), and moisture content ( $p=0.032$ ) and MOR were significantly correlated with moisture content ( $p=0.027$ ). In principle, the MOE and MOR correlate with wood moisture content between 8% and fibre saturation (about 30%). After this point, the correlations with moisture content may be spurious. Consequently, thicker and older stem logs were more rigid. In contrast, the coarse root sections have no significant correlations with wood properties.

Because Japanese black pine trees grow under difficult environmental conditions, their crown forms are often asymmetrical. Since it is assumed the stem logs were tapered cylinders (for purposes of computation), it is possible that this has led to the insignificant correlations between MOE and MOR for stem logs. Further, branch knots on the stem would influence MOR estimates and reduce MOR (Ruel et al. 2010; Gardiner et al. 2016). The knot factor (fknot) (Gardiner et al. 2000) should be considered to obtain better MOR estimates of the stem logs.

### Critical tsunami water depth

The numerical simulations revealed that the critical tsunami water depth varied with tree shape (Fig. 6). The critical tsunami water depth was greater for taller trees.

**Table 4** Correlation coefficients among wood properties

	Cambial age	$D_m$	$\tau$	ARW	$\rho_{W\_fresh}$	$\rho_{W\_dry}$	MC	MOE
<i>Stem</i>								
$D_m$	0.940***							
$\tau$	0.541*	0.450 <sup>ns</sup>						
ARW	-0.483 <sup>ns</sup>	-0.261 <sup>ns</sup>	-0.386 <sup>ns</sup>					
$\rho_{W\_fresh}$	-0.270 <sup>ns</sup>	-0.196 <sup>ns</sup>	-0.225 <sup>ns</sup>	0.146 <sup>ns</sup>				
$\rho_{W\_dry}$	-0.107 <sup>ns</sup>	-0.111 <sup>ns</sup>	0.011 <sup>ns</sup>	0.043 <sup>ns</sup>	0.861***			
MC	-0.281 <sup>ns</sup>	-0.171 <sup>ns</sup>	-0.186 <sup>ns</sup>	0.386 <sup>ns</sup>	0.032 <sup>ns</sup>	-0.389 <sup>ns</sup>		
MOE	0.738**	0.700**	0.454 <sup>ns</sup>	-0.125 <sup>ns</sup>	-0.361 <sup>ns</sup>	-0.036 <sup>ns</sup>	-0.561*	
MOR	-0.050 <sup>ns</sup>	-0.064 <sup>ns</sup>	0.361 <sup>ns</sup>	0.004 <sup>ns</sup>	-0.139 <sup>ns</sup>	0.132 <sup>ns</sup>	-0.575*	0.450 <sup>ns</sup>
<i>Root</i>								
$D_m$	0.905***							
$\tau$	-0.452 <sup>ns</sup>	-0.119 <sup>ns</sup>						
ARW	0.190 <sup>ns</sup>	0.429 <sup>ns</sup>	0.310 <sup>ns</sup>					
$\rho_{W\_fresh}$	0.119 <sup>ns</sup>	0.214 <sup>ns</sup>	-0.190 <sup>ns</sup>	0.595 <sup>ns</sup>				
$\rho_{W\_dry}$	-0.333 <sup>ns</sup>	-0.214 <sup>ns</sup>	0.190 <sup>ns</sup>	0.643 <sup>ns</sup>	0.595 <sup>ns</sup>			
MC	0.476 <sup>ns</sup>	0.524 <sup>ns</sup>	-0.333 <sup>ns</sup>	0.381 <sup>ns</sup>	0.762*	-0.024 <sup>ns</sup>		
MOE	-0.143 <sup>ns</sup>	-0.071 <sup>ns</sup>	0.190 <sup>ns</sup>	-0.119 <sup>ns</sup>	-0.214 <sup>ns</sup>	-0.214 <sup>ns</sup>	0.048 <sup>ns</sup>	
MOR	-0.286 <sup>ns</sup>	-0.095 <sup>ns</sup>	0.429 <sup>ns</sup>	-0.095 <sup>ns</sup>	-0.238 <sup>ns</sup>	0.048 <sup>ns</sup>	-0.262 <sup>ns</sup>	0.786*

$D_m$  mean diameter at the mid-span,  $\tau$ - taper, ARW average annual ring width,  $\rho_{W\_fresh}$  fresh wood density,  $\rho_{W\_dry}$  dry wood density, MC moisture content, MOE modulus of elasticity, MOR modulus of rupture

\* $p < 0.05$ ; \*\* $p < 0.01$ ; \*\*\* $p < 0.001$ , ns not significant at  $p < 0.05$

Critical tsunami water depth decreased with a higher Froude number because of greater  $u$  for the same tsunami water depth. The trees with  $H_{tr}/D_{BH}=50$  generally had higher resistance to tree breakage than uprooting; however, the difference was slight (Fig. 6a, c).

On the other hand, the trees with  $H_{tr}/D_{BH}=70$  exhibited a different relationship of resistance to tree breakage and uprooting (Fig. 6b, d). In general, the resistance to tree breakage was higher than uprooting when  $H_{tr} < 6$  m, whereas the opposite was true when  $H_{tr} > 8$  m. To clarify the difference, the modelled trees were subtracted with  $H_{tr}=4$  and 16 m (Fig. 7). The increase in  $H_{tr}/D_{BH}$  resulted in decreased resistance to uprooting and tree breakage, but the resistance to tree breakage decreased more. Accordingly, taller trees with higher  $H_{tr}/D_{BH}$  values were more vulnerable to tree breakage than uprooting.

Shuto (1987) summarized the maximum inundation depth in five cases of large tsunamis from 1896 to 1983 in coastal forests of Japan. The observed tsunami depth at 43 sites ranged from 0.5 to  $> 10$  m. Critical tsunami water depth for the modelled trees of Japanese black pine was less than 6 m in this study, even for taller and

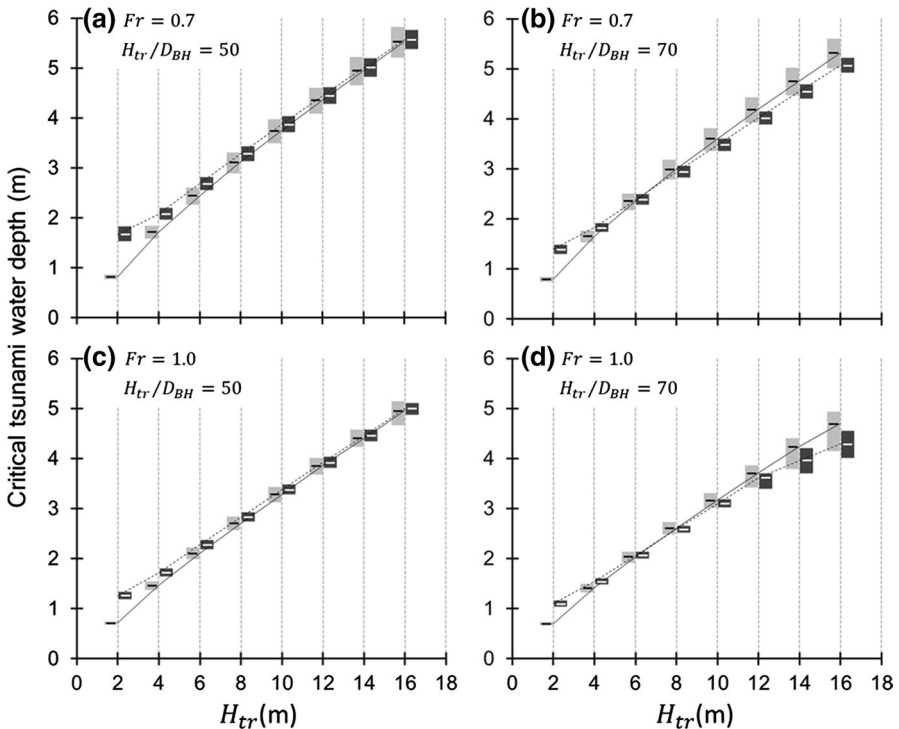


**Fig. 6** Critical tsunami water depth related to tree height ( $H_{tr}$ ) for uprooting (*bold line and light bar*) and stem breakage (*dashed line and dark bar*) for different  $H_{tr}/D_{BH}$  values and  $Fr$  (Froude number) of tsunamis. For uprooting, the range of the floating bar is calculated using the critical turning moment from Eq. 26 and a range of  $\pm 30\%$ , respectively. For stem breakage, the range of the floating bar is calculated by median and 5th and 95th percentile values of MOR, respectively



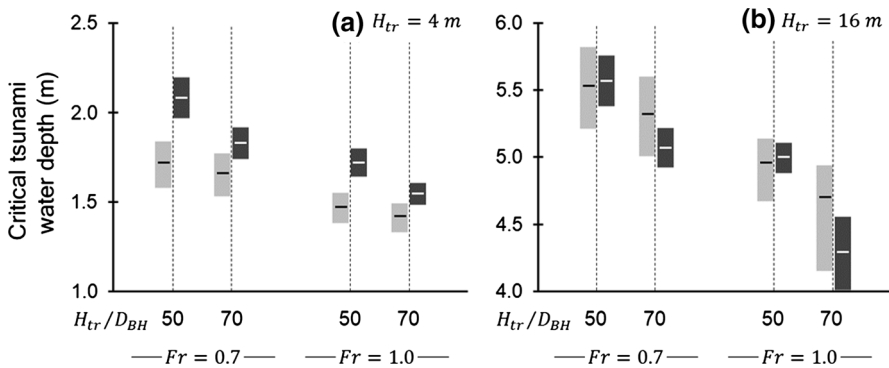


**Fig. 7** Critical tsunami water depth related to  $H_{tr}/D_{BH}$  and  $Fr$  for uprooting (light bar) and stem breakage (dark bar) for different tree heights ( $H_{tr}$ ) subtracted from Fig. 5

larger diameter trees (Fig. 6). Large tsunamis could destroy most of Japanese black pine trees; however, trees taller than 6 m can resist against tsunamis with water depth  $< 2$  m. Thus, these trees can contribute to mitigating the force of tsunamis.

From the numerical simulation, the resistance to uprooting was, in general, lower than the resistance to stem breakage regardless of tree size (Fig. 6). This finding is substantiated by direct field observations from the huge tsunami caused by the Great East Japan Earthquake in 2011 where more Japanese black pine trees experienced uprooting than stem breakage in coastal areas (Sato et al. 2012). The risk of uprooting is usually higher than stem breakage for smaller trees because smaller trees have less sufficiently developed root systems and smaller root-soil plate anchorage. The current findings indicate that the increase in root-soil plate anchorage due to the increase in tree size was less consequential for Japanese black pine trees on coastal sand dunes. Even though Japanese black pine is a typically deep-rooted tree species (Karizumi 2010), high groundwater levels in some coastal substrates could disturb the deep extension of roots, thereby lowering root-soil plate anchorage (FFPRI 2015). For the present trees, the tree-pulling test had a higher  $M_{C_{uproot}}$  than that estimated by Eq. 25 (Fig. 5a) because they had relatively larger diameters and root clump depths (Table 1). Tree #1, which experienced stem breakage, had the largest root depth of 3.2 m (Table 1). Although it is not known how large the root clumps of Japanese black pine trees were in previous studies, deep extension of root clumps would increase  $M_{C_{uproot}}$  of Japanese black pine more than the estimation by Eqs. 25 and 26. Additionally, it is important to increase stem thickness.

## Conclusion

This is the first study to estimate the resistance of Japanese black pine trees on coastal sand dunes by employing both numerical simulation and physical measurements of the critical turning moment to uprooting and stem bending strength. The regression equation for the critical turning moment to uprooting, computed

MOE and MOR values, and the numerical simulation method should be useful to those in the wood science community as well as coastal managers who need to know the mechanical strength of Japanese black pine to help evaluate their resistance against tsunamis. When tree height is same, lower  $H_{tr}/D_{BH}$  trees (i.e. thicker trees) have a greater critical tsunami water depth. Adequate forest thinning to increase  $D_{BH}$  is important to increase the resistance of Japanese black pine trees to tree damage by tsunamis. Accordingly, those Japanese black pine forests along the coast with larger trees and with low  $H_{tr}/D_{BH}$  values and deep root clumps are the best able to buffer the adverse impacts of tsunamis and resist against tsunami-induced tree damage. To increase the accuracy of the numerical simulation, additional studies are necessary to measure actual root-soil plate properties, consider soil conditions and to obtain better MOE and MOR values of the stem logs with the knot factor (fknot).

**Acknowledgements** We would like to thank the Ishikawa District Forest Office, Forest Agency, Ministry of Agriculture, Forestry and Fisheries, Japan. This study was partially supported by “Science and technology research promotion program for agriculture, forestry, fisheries and food industry” of the Agriculture, Forestry and Fisheries Research Council, research Grant #201412 of the Forestry and Forest Products Research Institute (FFPRI) and FFPRI Encouragement Model in Support of Researchers with Family Responsibilities. We gratefully acknowledge a Japan Society for the Promotion of Science (JSPS) Invitation Fellowship for Research in Japan (S16088: invitation of D.F. Levia by Dr. Kazuki Nanko) that aided the preparation of this manuscript. We are grateful to Dr. Takayuki Ito (FFPRI) for his assistance with the pulling test and Mr. Noboru Yamada (Ishikawa Agricultural and Forestry Research Center) for assistance with the bending test. We are grateful to Dr. Kana Kamimura (Shinshu University, Japan) for information on previous and related studies.

## References

- Achim A, Ruel J-C, Gardiner BA, Laflamme G, Meunier S (2005) Modelling the vulnerability of balsam fir forests to wind damage. For Ecol Manag 204:37–52. <https://doi.org/10.1016/j.foreco.2004.07.072>
- Auty D, Achim A (2008) The relationship between standing tree acoustic assessment and timber quality in Scots pine and the practical implications for assessing timber quality from naturally regenerated stands. Forestry 81:475–487. <https://doi.org/10.1093/forestry/cpn015>
- Bascuñán A, Moore JR, Walker JCF (2006) Variations in the dynamic modulus of elasticity with proximity to the stand edge in radiata pine stands on the Canterbury Plains, New Zealand. N Z J For 51:4–8
- Bruce D (1972) Some transformations of the Behre equation of tree form. For Sci 18:164–166
- Cannell MGR, Morgan J (1989) Branch breakage under snow and ice loads. Tree Physiol 5:307–317. <https://doi.org/10.1093/treephys/5.3.307>
- Coutts MP (1986) Components of tree stability in Sitka spruce on peaty gley soil. Forestry 59:173–197. <https://doi.org/10.1093/forestry/59.2.173>
- Cucchi V, Meredieu C, Stokes A et al (2004) Root anchorage of inner and edge trees in stands of Maritime pine (*Pinus pinaster* Ait.) growing in different podzolic soil conditions. Trees 18:460–466. <https://doi.org/10.1007/s00468-004-0330-2>
- Danielsen F, Sorensen MK, Olwig MF et al (2005) The Asian tsunami: a protective role for coastal vegetation. Science 310:643. <https://doi.org/10.1126/science.1118387>
- Dengler L, Preuss J (2003) Mitigation lessons from the July 17, 1998 Papua New Guinea tsunami. Pure Appl Geophys 160:2001–2031. <https://doi.org/10.1007/s00024-003-2417-x>
- Federal Emergency Management Agency (2012) Guidelines for design of structures for vertical evacuation from tsunamis. FEMA 646 Report. Applied Technology Council, California
- Forbes K, Broadhead J (2007) The role of coastal forests in the mitigation of tsunami impacts. Food and Agriculture Organization of the United Nations, Regional Office for Asia and the Pacific, Bangkok


- Forest Products Laboratory (1999) Wood handbook—wood as an engineering material. Gen Tech Rep FPL–GTR–113. U.S. Department of Agriculture, Forest Service, Forest Products Laboratory, Madison, WI
- Forestry and Forest Products Research Institute (FFPRI) (2015) Regeneration of coastal forests affected by tsunami. Tohoku Research Center, Morioka
- Fukami Y, Kitahara H, Ono H, Todo C, Yamase K (2011) Tree-pulling experiments under different conditions of soil water etc. *J Jpn For Soc* 93:8–13. <https://doi.org/10.4005/jjfs.93.8> (in Japanese with English summary)
- Gardiner B, Peltola H, Kellomäki S (2000) Comparison of two models for predicting the critical wind speeds required to damage coniferous trees. *Ecol Model* 129:1–23. [https://doi.org/10.1016/S0304-3800\(00\)00220-9](https://doi.org/10.1016/S0304-3800(00)00220-9)
- Gardiner B, Berry P, Moulia B (2016) Review: wind impacts on plant growth, mechanics and damage. *Plant Sci* 245:94–118. <https://doi.org/10.1016/j.plantsci.2016.01.006>
- Hollinger DY (1986) Herbivory and the cycling of nitrogen and phosphorus in isolated California oak trees. *Oecologia* 70:291–297. <https://doi.org/10.1007/BF00379254>
- Ido H, Nagao H, Kato H, Miura S (2013) Strength properties and effect of moisture content on the bending and compressive strength parallel to the grain of sugi (*Cryptomeria japonica*) round timber. *J Wood Sci* 59:67–72. <https://doi.org/10.1007/s10086-012-1297-z>
- Imai K, Suzuki A (2005) A method based on the pipe model for estimating the surface area and volume of coastal forest trees, and their lodging resistance. *Ann J Hydraul Eng* 49:859–864 (in Japanese with English summary)
- Imai K, Harada K, Minami Y, Kawaguchi S, Niinomiya E (2013) Advanced evaluation method for tsunami resistance of coastal tree. *J Jpn Soc Civil Eng Ser B2(69)*:361–365 (in Japanese with English summary)
- Kamimura K, Kitagawa K, Saito S, Mizunaga H (2012) Root anchorage of hinoki (*Chamaecyparis obtuse* (Sieb. Et Zucc.) Endl.) under the combined loading of wind and rapidly supplied water on soil: analyses based on tree-pulling experiments. *Eur J For Res* 131:219–227. <https://doi.org/10.1007/s10342-011-0508-2>
- Karizumi N (2010) The latest illustrations of tree roots. Seibundo Shinkosha, Tokyo (in Japanese)
- Kato A, Nakatani H (2000) An approach for estimating resistance of Japanese cedar to snow accretion damage. *For Ecol Manag* 135:83–96. [https://doi.org/10.1016/S0378-1127\(00\)00300-5](https://doi.org/10.1016/S0378-1127(00)00300-5)
- Kimmins JP (1972) Relative contributions of leaching, litter-fall, and defoliation by Neodiprion sertifer (Hymenoptera) to the removal of cesium-134 from red pine. *Oikos* 23:226–234. <https://doi.org/10.2307/3543410>
- Kinar NJ, Pomeroy JW (2015) Measurement of the physical properties of the snowpack. *Rev Geophys* 53:481–544. <https://doi.org/10.1002/2015RG000481>
- Koizumi A (1987) Studies on the estimation of the mechanical properties of standing trees by non-destructive bending test. *Res Bull Hokkaido Univ For* 44:1329–1415 (in Japanese with English summary)
- Kondo K, Koyama M, Nonoda T, Hayashi S (2006) Resistance of root system of Japanese black pine for external force assumed tsunami. *Trans Jpn For Soc* 117:G03 (in Japanese)
- Konta F (2001) The present conditions and functions of the coastal forests in Japan. *J Jpn Soc Coast For* 1:1–4 (in Japanese with English summary)
- Leban J-M, Haines DW (1999) The modulus of elasticity of hybrid larch predicted by density, rings per centimeter, and age. *Wood Fiber Sci* 31:394–402
- Lemon PC (1961) Forest ecology of ice storms. *J Torrey Bot Club* 88:21–29. <https://doi.org/10.2307/2482410>
- Merrill S (1948) Breakage of tung trees by hurricane winds in relation to variety, pruning method, and crop. *Proc Am Soc Hortic Sci* 51:145–151
- Miyata K, Kitahara A, Ono H (2013) Tree pulling test of Japanese black pine in Irigo Cape in Aichi Prefecture. *Chubu For Res* 61:1–4 (in Japanese)
- Morgan J, Cannell MGR (1987) Structural analysis of tree trunks and branches: tapered cantilever beams subject to large deflections under complex loading. *Tree Physiol* 3:365–374. <https://doi.org/10.1093/treephys/3.4.365>
- Murai H, Ishikawa M, Endo O, Tadaki Y (1992) Japanese coastal forest—Multi-faceted environmental functions and their utilization. Soft Science, Tokyo (in Japanese)
- Nakashima Y, Okada M (2011) Symbiosis with coastal forest. Yamagata Univ Press, Yamagata (in Japanese)

- Nicoll BC, Achim A, Mochan S, Gardiner BA (2005) Does steep terrain influence tree stability? A field investigation. *Can J For Res* 35:2360–2367. <https://doi.org/10.1139/x05-157>
- Nicoll BC, Gardiner BA, Rayner B, Peace AJ (2006) Anchorage of coniferous trees in relation to species, soil type, and rooting depth. *Can J For Res* 36:1871–1883. <https://doi.org/10.1139/X06-072>
- Nock CA, Lecigne B, Taugourdeau O et al (2016) Linking ice accretion and crown structure: towards a model of the effect of freezing rain on tree canopies. *Ann Bot* 117:1163–1173. <https://doi.org/10.1093/aob/mcw059>
- Noguchi H, Sato H, Torita H et al (2012) Numerical simulation of effect of inundation flow caused by the 2011 Tohoku earthquake tsunami on the *Pinus thunbergii* coastal forest: a case study of Misawa City of the Aomori Prefecture. *J Jpn Soc Coast For* 11:47–51 (in Japanese with English summary)
- Noguchi H, Suzuki S, Nanko K et al (2014) Evaluation of lodging resistance characteristics of broad-leaved tree and *Pinus thunbergii* planted in coastal sand dunes using tree-pulling experiments. *J Jpn Soc Coast For* 13:59–66 (in Japanese with English summary)
- Oda T (2003) People who made the coastal forest. Hokuto, Tokyo (in Japanese)
- Ono K, Ishikawa H (2012) Test and discussion on lodging resistance of coastal forest. *Trans Erosion Control Res* 51:152–157 (in Japanese)
- Peltola H, Kellomäki S, Väisänen H, Ikonen V-P (1999) A mechanistic model for assessing the risk of wind and snow damage to single trees and stands of Scots pine, Norway spruce, and birch. *Can J For Res* 29:647–661. <https://doi.org/10.1139/x99-029>
- Peltola H, Kellomäki S, Hassinen A, Granander M (2000) Mechanical stability of Scots pine, Norway spruce and birch: an analysis of tree-pulling experiments in Finland. *For Ecol Manag* 135:143–153. [https://doi.org/10.1016/S0378-1127\(00\)00306-6](https://doi.org/10.1016/S0378-1127(00)00306-6)
- Peterson CJ, Claassen V (2013) An evaluation of the stability of *Quercus lobata* and *Populus fremontii* on river levees assessed using static winching tests. *Forestry* 86:201–209. <https://doi.org/10.1093/forestry/cps080>
- Pretzsch H, Rais A (2016) Wood quality in complex forests versus even-aged monocultures: review and perspectives. *Wood Sci Technol* 50:845–880. <https://doi.org/10.1007/s00226-016-0827-z>
- Rossetto T, Peiris N, Pomonis A et al (2007) The Indian Ocean tsunami of December 26, 2004: observations in Sri Lanka and Thailand. *Nat Hazards* 42:105–124. <https://doi.org/10.1007/s11069-006-9064-3>
- Ruel J-C, Achim A, Herrera RE, Cloutier A (2010) Relating mechanical strength at the stem level to values obtained from defect-free wood samples. *Trees* 24:1127–1135. <https://doi.org/10.1007/s00468-010-0485-y>
- Sato H, Torita H, Masaka K et al (2012) Relationship between treefall damage and forest structure of *Pinus thunbergii* coastal forest by the 2011 Tohoku earthquake tsunami disaster: an example of Misawa City of Aomori Prefecture. *J Jpn Soc Coast For* 11:41–45 (in Japanese with English summary)
- Sattler DF, Comeau PG, Achim A (2014) Within-tree patterns of wood stiffness for white spruce (*Picea glauca*) and trembling aspen (*Populus tremuloides*). *Can J For Res* 44:162–171. <https://doi.org/10.1139/cjfr-2013-0150>
- Sawada M (1983) Transformation of tree trunk caused by wind and snow load. *Res Mater Hokkaido Branch FFPRI* 128:1–18 (in Japanese)
- Schmidt RA, Pomeroy JW (1990) Bending of a conifer branch at subfreezing temperatures: implications for snow interception. *Can J For Res* 20:1250–1253. <https://doi.org/10.1139/x90-165>
- Seischab FZ, Bernard JM, Eberle MD (1993) Glaze storm damage to western New York forest communities. *J Torrey Bot Club* 120:64–72. <https://doi.org/10.2307/2996665>
- Shuto N (1987) The effectiveness and limit of tsunami control forests. *Coast Eng Jpn* 30:143–153. <https://doi.org/10.1080/05785634.1987.11924470>
- Silins U, Lieffers VJ, Bach L (2000) The effect of temperature on mechanical properties of standing lodgepole pine trees. *Trees* 14:424–428. <https://doi.org/10.1007/s004680000065>
- Suzuki S, Sakamoto T, Noguchi H (2016) Wind damage risk estimation for strip cutting under current and future wind conditions based on moment observations in a coastal forest in Japan. *J For Res* 21:223–234. <https://doi.org/10.1007/s10310-016-0539-0>
- Tanaka T, Nagao H, Nakai T (1994) NDE of bending strength of Sugi logs. In: *Proc Int Conf Wood Poles Piles*, pp 112–136
- Tanaka N, Yagisawa J, Yasuda S (2013) Breaking pattern and critical breaking condition of Japanese pine trees on coastal sand dunes in huge tsunami caused by Great East Japan Earthquake. *Nat Hazards* 65:423–442. <https://doi.org/10.1007/s11069-012-0373-4>

- R Core Team (2016) R: a language and environment for statistical computing. R Foundation for Statistical Computing, Vienna, Austria. <http://www.R-project.org/>
- Todo C, Yamase K, Tanikawa T, Ohashi M, Ikeno H, Dannoura M, Hirano Y (2015) Effect of thinning on the critical turning moment of Sugi (*Cryptomeria japonica* (L.f.) D. Don). *J Jpn Soc Reveget Tech* 41:308–314. <https://doi.org/10.7211/jjsrt.41.308> (in Japanese with English summary)
- Torita H, Sato H, Masaka K, Abe T, Noguchi H, Sakamoto T, Kimura K (2014) Evaluation of tsunami resistance of trees using a simple dynamics model. *J Jpn For Soc* 96:206–211. <https://doi.org/10.4005/jjfs.96.206> (in Japanese with English summary)
- Williams AP, Allen CD, Macalady AK et al (2013) Temperature as a potent driver of regional forest drought stress and tree mortality. *Nat Clim Chang* 3:292–297. <https://doi.org/10.1038/nclimate1693>

**Publisher's Note** Springer Nature remains neutral with regard to jurisdictional claims in published maps and institutional affiliations.

## Affiliations

Kazuki Nanko<sup>1</sup>  · Satoru Suzuki<sup>1</sup> · Hironori Noguchi<sup>2</sup> · Yoji Ishida<sup>3</sup> · Delphis F. Levia<sup>4,5</sup> · Akira Ogura<sup>6</sup> · Hiroaki Hagino<sup>2</sup> · Hiroshi Matsumoto<sup>3</sup> · Hiromi Takimoto<sup>7</sup> · Tomoki Sakamoto<sup>1</sup>

<sup>1</sup> Department of Disaster Prevention, Meteorology and Hydrology, Forestry and Forest Products Research Institute, Tsukuba, Ibaraki 305-8687, Japan

<sup>2</sup> Tohoku Research Center, Forestry and Forest Products Research Institute, Morioka, Iwate 020-0123, Japan

<sup>3</sup> Ishikawa Agricultural and Forestry Research Center, Forestry Experiment Station, Hakusan, Ishikawa 920-2114, Japan

<sup>4</sup> Department of Geography, University of Delaware, Newark, DE 19716-2541, USA

<sup>5</sup> Department of Plant and Soil Sciences, University of Delaware, Newark, DE 19716-2170, USA

<sup>6</sup> Kenou General Agriculture Forestry Office Ishikawa Prefecture, Kanazawa, Ishikawa 920-8204, Japan

<sup>7</sup> Minamikaga General Agriculture Forestry Office Ishikawa Prefecture, Komatsu, Ishikawa 923-0801, Japan